

# UC Merced

## UC Merced Previously Published Works

### Title

Conservation of beneficial microbes between the rhizosphere and the cyanosphere

### Permalink

<https://escholarship.org/uc/item/96r140tq>

### Journal

New Phytologist, 240(3)

### ISSN

0028-646X

### Authors

Zheng, Qing

Hu, Yuntao

Kosina, Suzanne M

et al.

### Publication Date

2023-11-01

### DOI

10.1111/nph.19225

### Copyright Information

This work is made available under the terms of a Creative Commons Attribution License, available at <https://creativecommons.org/licenses/by/4.0/>

Peer reviewed

# Conservation of beneficial microbes between the rhizosphere and the cyanosphere

Qing Zheng<sup>1</sup> , Yuntao Hu<sup>1</sup> , Suzanne M. Kosina<sup>1</sup> , Marc W. Van Goethem<sup>1</sup> , Susannah G. Tringe<sup>1,2</sup> , Benjamin P. Bowen<sup>1,2</sup>  and Trent R. Northen<sup>1,2</sup> 

<sup>1</sup>Environmental Genomics and Systems Biology Division, Lawrence Berkeley National Laboratory, Berkeley, CA 94720, USA; <sup>2</sup>Joint Genome Institute, Berkeley, CA 94720, USA

## Summary

Author for correspondence:  
Trent R. Northen  
Email: [trnorthen@lbl.gov](mailto:trnorthen@lbl.gov)

Received: 12 February 2023  
Accepted: 26 July 2023

New Phytologist (2023) 240: 1246–1258  
doi: 10.1111/nph.19225

**Key words:** biocrusts, *Brachypodium distachyon*, cyanosphere, exometabolomics, microbiome recruitment, *Microcoleus vaginatus*, plant growth-promoting bacteria (PGPB), rhizosphere.

- Biocrusts are phototroph-driven communities inhabiting arid soil surfaces. Like plants, most photoautotrophs (largely cyanobacteria) in biocrusts are thought to exchange fixed carbon for essential nutrients like nitrogen with cyanosphere bacteria. Here, we aim to compare beneficial interactions in rhizosphere and cyanosphere environments, including finding growth-promoting strains for hosts from both environments.
- To examine this, we performed a retrospective analysis of 16S rRNA gene sequencing datasets, host–microbe co-culture experiments between biocrust communities/biocrust isolates and a model grass (*Brachypodium distachyon*) or a dominant biocrust cyanobacterium (*Microcoleus vaginatus*), and metabolomic analysis.
- All 18 microbial phyla in the cyanosphere were also present in the rhizosphere, with additional 17 phyla uniquely found in the rhizosphere. The biocrust microbes promoted the growth of the model grass, and three biocrust isolates (*Bosea* sp.\_L1B56, *Pseudarthrobacter* sp.\_L1D14 and *Pseudarthrobacter picheli*\_L1D33) significantly promoted the growth of both hosts. Moreover, pantothenic acid was produced by *Pseudarthrobacter* sp.\_L1D14 when grown on *B. distachyon* exudates, and supplementation of plant growth medium with this metabolite increased *B. distachyon* biomass by over 60%.
- These findings suggest that cyanobacteria and other diverse photoautotrophic hosts can be a source for new plant growth-promoting microbes and metabolites.

## Introduction

Biological soil crusts (biocrusts) are photoautotroph-dominated soil surface communities dwelling in many low-productivity ecosystems such as drylands and cover *c.* 12% of the terrestrial surface (Rodríguez-Caballero *et al.*, 2018). These surface communities provide multiple critical ecosystem functions such as stabilizing the surface of bare soil, retaining soil moisture, and capturing nutrients; these functions vary depending on the successional stage (Elbert *et al.*, 2012; Strauss *et al.*, 2012; Belnap *et al.*, 2016; Chamizo *et al.*, 2016). Early-succession biocrusts (light crusts, less mature) were formed when pioneer primary producers (typically filamentous cyanobacteria such as *Microcoleus vaginatus*) colonize bare ground of drylands through the production of exopolysaccharides that bind soil particles (García-Pichel & Wojciechowski, 2009). By analogy to a plant rhizosphere, photoautotrophic cyanobacteria were suggested to shape heterotrophic bacteria around it, forming a cyanosphere (Couradeau *et al.*, 2019). Recent studies of ‘core microbiomes’ have shown that root-associated bacterial communities share common features not only between different accessions of the same plant species but also across whole groups of plants (Engelbrekton *et al.*, 2012; Hamonts *et al.*, 2018; Xu *et al.*,

2018) and even with algae (Durán *et al.*, 2022). These shared common features may extend to biocrust cyanobacteria, since they are also phototrophic hosts like algae. Interestingly, bacterial phyla including *Proteobacteria*, *Actinobacteriota*, *Bacillota*, and *Bacteroidota* that were commonly recognized as taxonomic core microbiomes associated with plant roots (Engelbrekton *et al.*, 2012; Coleman-Derr *et al.*, 2016; Lemanceau *et al.*, 2017; Yeoh *et al.*, 2017; Durán *et al.*, 2022) were also found in biocrust ‘cyanosphere’ communities (da Rocha *et al.*, 2015; Couradeau *et al.*, 2019).

Host exudation of metabolites is another commonality between the ‘cyanosphere’ and the region surrounding plant roots (i.e. the rhizosphere). Indeed, studies have shown that plants and a filamentous cyanobacterium found in biocrusts both secrete exudates to recruit microbiomes in exchange for nutrients (Baran *et al.*, 2015; Swenson *et al.*, 2018; Couradeau *et al.*, 2019). For plants, this impact of exudation on the rhizosphere microbiome and the surrounding rhizosphere soil is known as the rhizosphere effect (Sasse *et al.*, 2018). For instance, aromatic acids, benzoxazinoids, flavonoids, glucosinolates and *p*-coumaric acid have been previously found to play important roles in rhizosphere assemblies (Bressan *et al.*, 2009; Abdel-Lateif *et al.*, 2012; Zhou & Wu, 2012; Hu *et al.*, 2018; Zhalnina *et al.*, 2018; Kudjordjie

*et al.*, 2019). In the diazotroph-enriched cyanosphere associated with the prominent non-nitrogen-fixing biocrust cyanobacterium *M. vaginatus* (Couradeau *et al.*, 2019), a symbiotic relationship between *M. vaginatus* and its cyanosphere based on a carbon for nitrogen nutrient exchange has also been reported in recent studies (Nelson & Garcia-Piche, 2021; Nelson *et al.*, 2021).

Biocrusts are thought to be similar in composition and structure to the soil communities and coexist with plants across drylands (Belnap *et al.*, 2016; Havrilla *et al.*, 2019). Previous studies have shown that biocrust could affect plant growth by mediating soil environment such as soil structure, fertility, and microclimate (Belnap, 2006; Concostrina-Zubiri *et al.*, 2013; Tucker *et al.*, 2017). Although some studies found neutral or negative effects of biocrust communities on plant performances previously, biocrusts have been reported to facilitate plant growth world-wide (Lesica & Shelly, 1992; DeFalco *et al.*, 2001; Zhang & Nie, 2011; Havrilla *et al.*, 2019), suggesting there might be some beneficial interactions between biocrust communities and plants. Given similarities in community structures and recruitment processes between plants and biocrust photoautotrophic cyanobacteria, we hypothesize that some biocrust microbes that benefit cyanobacterial hosts might also benefit plants. To investigate this, we first compared the rhizosphere and biocrust cyanosphere microbiomes by retrieving and analyzing 16S rRNA gene sequencing datasets from previous studies (see the [Materials and Methods](#) section). We then used an inoculation experiment and 16S rRNA gene sequencing to examine host recruitment of biocrust communities by both the model grass *Brachypodium distachyon* and the predominant biocrust cyanobacterium *M. vaginatus*. We observed a host growth-promoting effect of biocrust bacteria, which we further explored with an inoculation experiment between biocrust isolates and *B. distachyon* or *M. vaginatus*. Exometabolite profiles of biocrust isolates grown on exudates of both *B. distachyon* root and *M. vaginatus* were then used to unravel possible underlying mechanisms for host growth-promoting effects.

## Materials and Methods

### Retrospective analysis of 16S rRNA gene sequencing data

To compare microbiomes recruited to the rhizosphere and the cyanosphere, we first retrieved, reprocessed, and reanalyzed raw 16S rRNA gene amplicon sequencing data (i.e. FASTQ) collected from previous studies (Supporting Information Table S1). To minimize the bias induced by different sequencing platforms and primers, we only included a limited set of studies in which 16S-V4 regions of the 16S rRNA gene were amplified using 515-F and 806-R primer pairs and sequenced on the Illumina MiSeq platform. Here, we included studies for the cyanosphere of *M. vaginatus* and the rhizosphere of six types of grass (i.e. *Bromus inermis*, *Oryza sativa*, *Phalaris arundinacea*, *Phleum pratense*, *Sporobolus cryptandrus*, and *Sporobolus neglectus*) from Poaceae family. The paired-end MiSeq reads were demultiplexed, filtered, and then processed into merged amplicon sequencing variants (ASVs) using the DADA2 pipeline (v.1.16; Callahan *et al.*,

2016). The ASVs were aligned to the SILVA SSU database (v.138) for a taxonomic assignment using the naïve Bayesian classifier (Wang *et al.*, 2007) implemented by DADA2. All datasets were subsampled at an even depth of 500 reads to retain as many datasets as possible.

### Biocrust sample collection and storage

Biocrusts were cored and collected with multiple Petri dishes (6 cm<sup>2</sup> × 1 cm depth) from Dinosaur Mountain (38°42'55"N, 109°41'33"W; Moab, UT, USA) in October 2018. Samples were collected along a maturity gradient of cyanobacteria-dominated biocrusts ranging from light, young to darker, mature (Swenson *et al.*, 2018). Samples were brought back to Lawrence Berkeley National Laboratory at ambient temperature and stored in a dark desiccation chamber, conditions that are known to support long-term viability. For this study, light biocrusts from an early successional stage were used as a source of heterotrophic bacteria for plant and cyanobacterial colonization.

### *Brachypodium distachyon* and *M. vaginatus* growth conditions

Seeds of the model grass *B. distachyon* Bd21-3 (Vogel & Hill, 2008) were dehusked and surface sterilized in 20% v/v sodium hypochlorite for 30 s and in 70% v/v ethanol for 5 min, followed by five rinses with sterile water. After being stratified for 3 d at 4°C in the dark, *B. distachyon* seedlings were germinated on 0.2× Murashige & Skoog (MS) basal salt mixture (PhytoTech Labs, Lenexa, KS, USA) with 1% agar (Bio-World, Dublin, OH, USA) plates in a 16 h : 8 h, light : dark regime at 24°C. The MS medium used to cultivate *B. distachyon* contains major salts and trace metals. Fabricated ecosystems (EcoFABs; Gao *et al.*, 2018) were sterilized, and seedlings were transferred to EcoFABs 5 d after germination. The EcoFABs were filled with 4 ml of 0.2× MS medium and incubated in a 16 h : 8 h, light : dark regime at 24°C with 150 μmol m<sup>-2</sup> s<sup>-1</sup> light intensity for 5 d before further processing.

The axenic cyanobacterium *M. vaginatus* PCC 9802 (4 ml) grown in 1× BG 11 medium (Sigma-Aldrich) was incubated in 12-well cell culture plates (Corning, Tewksbury, MA, USA) in a 12 h : 12 h, light : dark regime at 24°C, with 15 μmol m<sup>-2</sup> s<sup>-1</sup> light intensity for 5 d before further processing. The BG 11 medium used to cultivate *M. vaginatus* contains major salts and trace metals.

### The microbial inoculation on *B. distachyon* and *M. vaginatus*

To compare the biocrust microbiome recruited to *M. vaginatus* and the root of *B. distachyon*, we inoculated *B. distachyon* and *M. vaginatus* with soil water from biocrusts. Three biological replicates of biocrust inoculum were prepared individually by stirring 2 g biocrust in 20 ml 0.85% NaCl solution (Sigma-Aldrich) at 24°C for 5 min and setting aside for 15 min, followed by filtration through an autoclaved 20 μm Whatman filter paper (Cytiva, Marlborough, MA, USA) to remove nematodes or micro-arthropods while retaining microorganisms (van de

Voorde *et al.*, 2012). Three replicates of filtered soil water samples were collected separately and added to three EcoFABs and three wells of a 12-well cell culture plate with a final OD<sub>600</sub> of 0.02 to inoculate three replicates of *B. distachyon* and *M. vaginatus*, respectively. Three replicates of uninoculated *M. vaginatus* were cultivated in three wells of the same 12-well cell culture plate as inoculated samples. The rest of the filtered soil water samples were centrifuged at 3000 *g* for 10 min, their supernatants were discarded, and the sediments were collected and stored at  $-80^{\circ}\text{C}$  before total DNA extraction. The uninoculated controls and the inoculated *B. distachyon* were then incubated in a 16 h : 8 h, light : dark regime at  $24^{\circ}\text{C}$  with  $150\ \mu\text{mol m}^{-2}\ \text{s}^{-1}$  light intensity for 5 d. Plant roots were subsequently collected by excision of the root from the shoot *c.* 5 mm below the rosette, followed by washing roots in 10 ml  $1\times$  PBS (Leinco Technologies, St Louis, MO, USA). Shoot tissues of each *B. distachyon* plant were collected separately from root tissues, and shoot and root biomass were both measured at harvest. The uninoculated controls and the inoculated *M. vaginatus* were incubated in a 12 h : 12 h, light : dark regime at  $24^{\circ}\text{C}$  with  $15\ \mu\text{mol m}^{-2}\ \text{s}^{-1}$  light intensity for 14 d. Chl*a* absorbance at 665 and 720 nm (Ritchie, 2006) was measured using a microplate reader (Biotek, Santa Clara, CA, USA) to assess biomass production by extracting 1 ml of *M. vaginatus* from each culture well. The rest of 3 ml *M. vaginatus* from each well was washed with  $1\times$  PBS and spun down, and pellets were collected for further analysis. The collected plant roots and *M. vaginatus* pellets were stored in Lysing Matrix E tubes (MP Biomedicals, Santa Ana, CA, USA) at  $-80^{\circ}\text{C}$  before total DNA extraction.

To further evaluate the host growth-promoting effect of biocrust bacteria, we selected a variety of biocrust bacterial isolates (Table 1) belonging to 3 phyla (*Actinobacteriota*, *Proteobacteria*, and *Bacillota*) from an existing isolate collection to inoculate the root of *B. distachyon* and *M. vaginatus*, respectively. These isolates were isolated from biocrusts in a previous study (da Rocha *et al.*, 2015). The biocrust samples used for isolation and this study were from the same location but collected at different times. Biocrust isolates that could grow in liquid medium were cultured to saturation ( $30^{\circ}\text{C}$ , 15 ml round-bottom Falcon tubes, shaken at 200 rpm) in 5 ml of  $1\times$  R2A medium (HiMedia Laboratories, Kennett Square, PA, USA) for 5 d, then spun down, and washed three times with  $1\times$  PBS before resuspending in  $1\times$  PBS. The OD<sub>600</sub> of each strain was determined using a plate reader (Biotek). Three replicates of *B. distachyon* grown in  $0.2\times$  MS medium and *M. vaginatus* grown in  $1\times$  BG11 medium were inoculated with resuspended biocrust isolates to a final composite OD<sub>600</sub> of 0.02. Biocrust isolates that could not grow in  $1\times$  R2A liquid medium were grown on  $1\times$  DIFCO™ R2A agar (BD Biosciences, San Jose, CA, USA) plates for 5 d, and a colony of each bacterium was washed three times with  $1\times$  PBS before inoculating the hosts. The uninoculated controls and the inoculated *B. distachyon* were grown for 14 d under a 16 h : 8 h, light : dark regime cycle,  $24^{\circ}\text{C}$  with  $150\ \mu\text{mol m}^{-2}\ \text{s}^{-1}$  light intensity until harvest. The shoot and root tissues of each plant were harvested separately to determine biomass. The uninoculated controls and the inoculated *M. vaginatus* were incubated in a

**Table 1** Selected biocrust isolates for co-culture experiment.

Biocrust isolates	Phylum	Genus/species	Closest ANI placement (%)
L1B01	<i>Actinobacteriota</i>	<i>Patulibacter</i> sp. L1B01	89.31
L1B27	<i>Actinobacteriota</i>	<i>Solirubrobacter</i> sp. D1B35	89.72
L1B36	<i>Actinobacteriota</i>	<i>Arthrobacter oryzae</i>	98.96
L1B40	<i>Proteobacteria</i>	<i>Paracraurococcus</i> sp. 1N-11	88.86
L1B44	<i>Actinobacteriota</i>	<i>Modestobacter versicolor</i>	99.15
L1B45	<i>Actinobacteriota</i>	<i>Williamsia muralis</i>	94.40
L1B56	<i>Proteobacteria</i>	<i>Bosea</i> sp. Leaf344	87.60
L1D06	<i>Actinobacteriota</i>	<i>Williamsia</i> sp. B3_4TCO2	97.22
L1D14	<i>Actinobacteriota</i>	<i>Pseudarthrobacter</i> sp.	87.17
L1D33	<i>Actinobacteriota</i>	<i>Pseudarthrobacter picheli</i> (also known as <i>Pseudarthrobacter phenanthrenivorans</i> Sphe3)	91.28
D1B11	<i>Bacillota</i>	<i>Bacillus mycoides</i>	97.34
D1B20	<i>Bacillota</i>	<i>Methylobacterium extorquens</i>	96.57
D1B50	<i>Proteobacteria</i>	<i>Belnapia moabensis</i>	97.29
D2B09	<i>Actinobacteriota</i>	<i>Kribbella flavida</i>	95.75
D2B23	<i>Actinobacteriota</i>	<i>Modestobacter versicolor</i>	99.11
D2B31	<i>Proteobacteria</i>	<i>Bradyrhizobium</i> sp003020075	99.99
D2B56	<i>Bacillota</i>	<i>Bacillus mycoides</i>	97.45
D2D21	<i>Actinobacteriota</i>	<i>Micromonospora</i> sp.	99.33

12 h : 12 h, light : dark regime at  $24^{\circ}\text{C}$  with  $15\ \mu\text{mol m}^{-2}\ \text{s}^{-1}$  light intensity for 14 d. Chl*a* fluorescence of 1 ml *M. vaginatus* samples from cell culture wells was determined to assess biomass production. After harvesting, the root tissues of each *B. distachyon* or 1 ml *M. vaginatus* were then washed using  $1\times$  PBS, and subsequently, an aliquot (15  $\mu\text{l}$ ) of the washed solution was spread onto  $1\times$  R2A agar plate and cultured under  $30^{\circ}\text{C}$  for 5 d to determine the survival of the isolates in the media in the presence of *B. distachyon* root or *M. vaginatus*. Bacterial colonies on these plates were compared to colonies without hosts to ensure that they originated from the same isolates.

### The effect of pantothenic acid on *B. distachyon* and *M. vaginatus*

To evaluate the growth-promoting effects of pantothenic acid on hosts, we cultivated three replicates of *B. distachyon* on  $0.2\times$  MS agar in Nunc Bioassay Dishes (Sigma-Aldrich) supplemented with 0.01  $\mu\text{M}$ , 0.1  $\mu\text{M}$ , 1  $\mu\text{M}$ , 0.01 mM, and 0.1 mM pantothenic acid (Sigma-Aldrich). The control plants were cultivated on a  $0.2\times$  MS agar dish. Meanwhile, three replicates of 4 ml *M. vaginatus* grown in  $1\times$  BG11 medium supplemented with 0.01  $\mu\text{M}$ , 0.1  $\mu\text{M}$ , 1  $\mu\text{M}$ , 0.01 mM, and 0.1 mM pantothenic acid were cultured in a 12-well cell culture plate. The control *M. vaginatus* grown in  $1\times$  BG11 medium were also cultured in the 12-well cell culture plate. After 28 d of cultivation, shoot and root biomass of *B. distachyon* was measured separately, and Chl*a* of 1 ml *M. vaginatus* was measured to estimate biomass production.

## DNA extraction, amplification, and sequencing data analysis

To compare the microbiome recruited to *B. distachyon* and *M. vaginatus* after inoculation by biocrust soil water, DNA of three replicates of frozen filtered soil inoculum, uninoculated controls and inoculated *B. distachyon* roots and *M. vaginatus* was extracted using the FastDNA™ SPIN Kit (MP Biomedicals) following the modified manufacturers' recommendations (Zheng *et al.*, 2019). Aliquots (1 µl) of DNA extracts were quantified with the Qubit dsDNA HS assay kit and Qubit 3.0 fluorometer (Invitrogen). DNA templates of each sample were sent to the Sequencing Core Facility at the La Jolla Institute for Immunology (San Diego, CA, USA) for library preparation and amplicon sequencing. Briefly, the V4 hypervariable region of the 16S rRNA gene (c. 291 bp) was amplified via polymerase chain reaction (PCR) with the modified 515-F (5' GTG CCA GCM GCC GCG GTA A 3') and modified 806-R (5' GGA CTA CHV GGG TWT CTA AT 3') primer pairs (Caporaso *et al.*, 2012). The library was prepared by adaptor ligation and PCR using the TruSeq Nano DNA Library Prep Kit (Illumina, San Diego, CA, USA) according to the TruSeq Nano protocol (FC-121-4003; Illumina). The MiSeq was run in the 2 × 250 cycle configuration using the MiSeq Reagent kit v3 (Illumina). The DADA2 (v.1.16) pipeline (Callahan *et al.*, 2016) was used to demultiplex paired-end MiSeq reads before processing into merged amplicon sequence variants (ASVs). The ASVs were aligned to the SILVA SSU database (v.138) for a taxonomic assignment using the naïve Bayesian classifier (Wang *et al.*, 2007) implemented by DADA2.

We performed whole-genome sequencing (WGS) of 18 bacterial isolates by extracting whole-genomic DNA (data are not available for *Arthrobacter oryzae*\_L1B36 and *Micromonospora* sp.\_D2D21 due to DNA contamination) from the isolate using MasterPure™ Gram Positive DNA Purification Kit (Lucigen, Middleton, WI, USA) following the manufacturers' recommendations. Aliquots (1 µl) of DNA extracts were subsequently quantified with the Qubit dsDNA HS assay kit and Qubit 3 fluorometer (Invitrogen). DNA template of the sample was sent to Novogene Corp. Inc. (Sacramento, CA, USA) for library preparation and WGS with Illumina NovaSeq 6000 instrument with PE150. The low-quality reads were filtered using PRINSEQ-LITE v.0.20.4, and the quality-corrected reads were assembled into contigs using SPADes v.3.15.5. The assembly qualities were then checked by CHECKM v.1.1.3 before the genomes were annotated using PROKKA v.1.14.6. Taxonomic assignments of the genomes were provided using the GTDB-Tk database v.1.0.2. We then performed a phylogenetic analysis of the isolates. The phylogenomic species tree (Fig. S1) of *Pseudarthrobacter phenanthrenivorans* Sphe3\_L1D33 was constructed using 49 core, universal genes defined by COG (Clusters of Orthologous Groups) domains. Closely related genomes were selected from public genomes on RefSeq. Genome relatedness was determined by an alignment similarity search to a selected subset of the 49 COG domains. The genomes were then used in a multiple sequence alignment (MSA) for each COG family. The curated alignments are trimmed using GBLOCKS to remove poorly aligned sections of

the MSA. Finally, the MSA was concatenated, and the phylogenetic tree was reconstructed using FASTTREE2 with maximum likelihood algorithm. The final tree was visualized in iTOL v.6.6. The closest reference strain was found to be *Pseudarthrobacter phenanthrenivorans* Sphe3\_L1D33 with an average nucleotide identity (ANI) of 91.28% ANI, indicating that it is a new species (Konstantinidis & Tiedje, 2005). Given its dramatic positive impact on plant growth (see the Results section) and its phylogenetic novelty, we name it *Pseudarthrobacter picheli*. 'Picheli' in recognition of Ferran Garcia-Pichel's important contributions to the field of biocrust research. The same methods were applied to determine the closest reference strains for the other 15 selected isolates (except for *Arthrobacter oryzae*\_L1B36 and *Micromonospora* sp.\_D2D21 due to DNA contamination). The 16S rRNA gene sequences of *Arthrobacter oryzae*\_L1B36 and *Micromonospora* sp.\_D2D21 were obtained from a previous study (da Rocha *et al.*, 2015). We then blasted sequences of these two isolates with the NCBI NR-database using BLAST online tool (<https://blast.ncbi.nlm.nih.gov/Blast.cgi>) for bacterial genus or species assignment. The highest identity was selected as the identified genus or species (Table 1).

## Metabolomic analysis

To further examine whether biocrust isolates excrete metabolites that potentially promote the growth of the hosts, we used a metabolomic approach to profile exometabolites of 18 biocrust isolates grown in hosts' exudates. Specifically, we germinated *B. distachyon* seeds on 0.2 × MS agar plates and transferred seedlings (three seedlings per container) to three autoclaved Microbox round containers (Sac O2, Deinze, Belgium) 5 d after germination. The Microboxes were filled with 300 ml 0.2 × MS medium and 1100 g 5 mm glass beads (VWR, Radnor, PA, USA). The *B. distachyon* were cultivated in a 16 h : 8 h, light : dark regime at 24°C with 150 µmol m<sup>-2</sup> s<sup>-1</sup> light intensity for 14 d with weekly medium change; plant root exudates were collected at 7- and 14-d intervals and pooled together. The *M. vaginatus* was cultivated in six 650 ml Cellstar suspension culture flasks (VWR) filled with 150 ml 1 × BG11 medium. All *M. vaginatus* were cultivated in a 12 h : 12 h, light : dark regime at 24°C, with 15 µmol m<sup>-2</sup> s<sup>-1</sup> light intensity for 14 d. Similar to *B. distachyon*, the growth medium was changed weekly, and the exudates of *M. vaginatus* were collected at 7- and 14-d intervals and combined. The pooled exudates (1800 ml) of *B. distachyon* or *M. vaginatus* were frozen, lyophilized, and then resuspended in 90 ml sterile water to prepare 20-fold concentrated exudates. Next, we cultured three replicates of individual biocrust isolates (30°C, 5 ml round-bottom Falcon tubes, shaken at 200 rpm) in the 20-fold concentrated exudates, which were collected from the root of *B. distachyon* or spent medium of *M. vaginatus*. We observed slow growth of these isolates in hosts' exudates, and no quantitative growth data were recorded. Isolates were cultivated for 14 d before collecting the spent medium. After 14 d of cultivation, 1 ml of each collected spent medium was filtered and immediately stored at -80°C before further analysis. The frozen spent media were further lyophilized and then resuspended in 1 ml of methanol, vortexed for

30 s, and sonicated in an ice water bath for 15 min. Methanol extracts were centrifuged at 9000 *g* for 3 min to remove insoluble salts, and the supernatants were dried using a SpeedVac Concentrator (Thermo Fisher Scientific, Waltham, MA, USA). The dried material was then resuspended in 150  $\mu$ l of methanol with  $^{13}\text{C}$ - and  $^{15}\text{N}$ -labeled internal standards and filtered through 0.22  $\mu$ m centrifuge tubes (Nanosep MF; Pall Co., NY, USA) before LC–MS/MS analysis. Polar metabolites were separated using Agilent 1290 series HPLC installed with an InfinityLab Poroshell 120 HILIC-Z, 2.1  $\times$  150 mm, 2.7  $\mu$ m column (683775-924; Agilent Technologies, Santa Clara, CA, USA). The MS data were acquired using a Q Exactive Hybrid Quadrupole-Orbitrap mass spectrometer (Thermo Fisher Scientific) in both positive and negative ionization modes. LC–MS/MS method parameters are defined in Table S2. The metabolomic data were analyzed using METATLAS toolbox (Bowen & Northen, 2010; Yao *et al.*, 2015) to obtain the extracted ion chromatography and peak height. Identification of metabolites (Table S3) was performed by comparing measured MS/MS fragmentation spectra, *m/z* values, and retention times with those of standard reference compounds analyzed using the same methods.

### Statistical data analysis

All statistical analyses were performed using R software v.3.6.1 (R Core Team, 2019). Kruskal–Wallis test and Dunn's test were applied to compare microbial relative abundance in the rhizosphere and the cyanosphere. The UpSet plot was made using the 'UPSETR' package to visualize intersections between bacterial/archaeal phyla found in the rhizosphere and the cyanosphere based on retrospective data analysis. The Welch's *t*-tests were applied to compare the growth-promoting effects of biocrust communities, isolates and pantothenic acid on the biomass production of hosts. Principal coordinates analysis (PCoA) based on Bray–Curtis dissimilarity was performed using 'VEGAN' package to visualize microbial communities (at ASV level) in the rhizosphere and the cyanosphere in the retrospective study, or in the biocrust inoculum and recruited to *B. distachyon* and *M. vaginatus* after inoculated by the biocrust soil water. Linear regression was performed to assess the correlation between biomass production of *B. distachyon* and *M. vaginatus* after being inoculated by biocrust isolates for 14 d. Metabolites detected in exudates of uninoculated *B. distachyon* and *M. vaginatus* were compared with medium control and extraction control by Tukey's HSD and were visualized in a dotplot. The exometabolites of biocrust isolates grown in hosts' exudates that were significantly different (if at least one sample group had an adjusted  $P < 0.05$  when compared to those of medium blanks with two-tailed *t*-tests) from the background were clustered based on Euclidean distance in heatmaps; all biocrust isolates were clustered based on Euclidean distance as well. Metabolite levels for individual bacterial exudates can be found in Table S3. Nonmetric multidimensional scaling (NMDS) ordinations based on Bray–Curtis dissimilarity were performed using 'VEGAN' package to visualize the dissimilarities in exometabolites of biocrust isolates grown in both hosts' exudates. The selection of candidate molecules for host growth promotion

was done by correlating the metabolite levels with the biomass of each host (Pearson  $R > 0.4$ ). All reported *P* values were corrected for multiple testing using the 'p.adjust' function (method = 'BH'; Benjamini & Hochberg, 1995) in R.

Amplicon libraries of the sequenced biocrust controls and inoculated hosts were rarefied to 974 sequences for bacteria/archaea analysis, to ensure even sampling depth and retain as many datasets as possible for microbial community relative abundance comparison. The alpha-diversity including microbial richness (i.e. Chao1) and diversity (i.e. Shannon) indices were analyzed using the 'PHYLOSEQ' package in R.

## Results

The rhizosphere contained all of the major phyla contained in the cyanosphere

To compare the microbiomes in rhizosphere environments with those in cyanosphere environments, we performed a retrospective analysis of published 16S rRNA gene sequencing data. A total of 51 116 989 16S rRNA gene sequences from 181 rhizosphere samples and 40 *M. vaginatus* cyanosphere samples were analyzed and classified into 210 742 distinct ASVs. After rarefying to identical sequence depth (500), we obtained 108 500 high-quality sequences forming 8739 ASVs that could be assigned to 35 phyla, and 620 genera (ASVs assigned to *M. vaginatus* were excluded from further analysis). We found significantly lower microbial richness and diversity in cyanosphere samples compared with rhizosphere samples (Chao1,  $P < 0.001$ ; Shannon,  $P < 0.001$ ; Fig. S2). Twelve phyla showed a relative abundance of  $> 1\%$  of the total bacterial/archaeal community in either rhizosphere or cyanosphere. Specifically, *Proteobacteria*, *Bacteroidota*, *Cyanobacteria*, *Acidobacteriota*, *Myxococcota*, *Actinobacteriota*, *Verrucomicrobiota*, *Planctomycetota*, *Chloroflexota*, *Gemmatimonadota*, *Bacillota*, and *Desulfobacterota* accounted for the largest proportion of sequences of bacterial/archaeal communities (Fig. 1a). Members of *Proteobacteria* were abundant in both the rhizosphere and the cyanosphere (Fig. 1a). Additionally, *Bacteroidota* and *Cyanobacteria* (excluding *M. vaginatus*) were found at higher relative abundances in the cyanospheres than in the rhizospheres, accounting for almost 50% of cyanosphere sequences but  $< 10\%$  of the rhizosphere, while more *Acidobacteria*, *Verrucomicrobiota*, and *Planctomycetota* were found in the rhizosphere. Interestingly, we found that all 18 phyla in the cyanosphere were also present in the rhizosphere, and 17 additional phyla were found in the rhizosphere but not in the cyanosphere (Fig. 1b; Table S4). While at higher taxonomy levels there are 18 shared phyla between the rhizosphere and the cyanosphere, there are substantial differences at the ASV level (Fig. S3).

### Analysis of recruitment of biocrust bacteria by *B. distachyon* and *M. vaginatus*

Given commonalities in the rhizosphere and the cyanosphere communities at the phylum level, we performed plant and cyanobacteria colonization experiments using the same biocrust soil

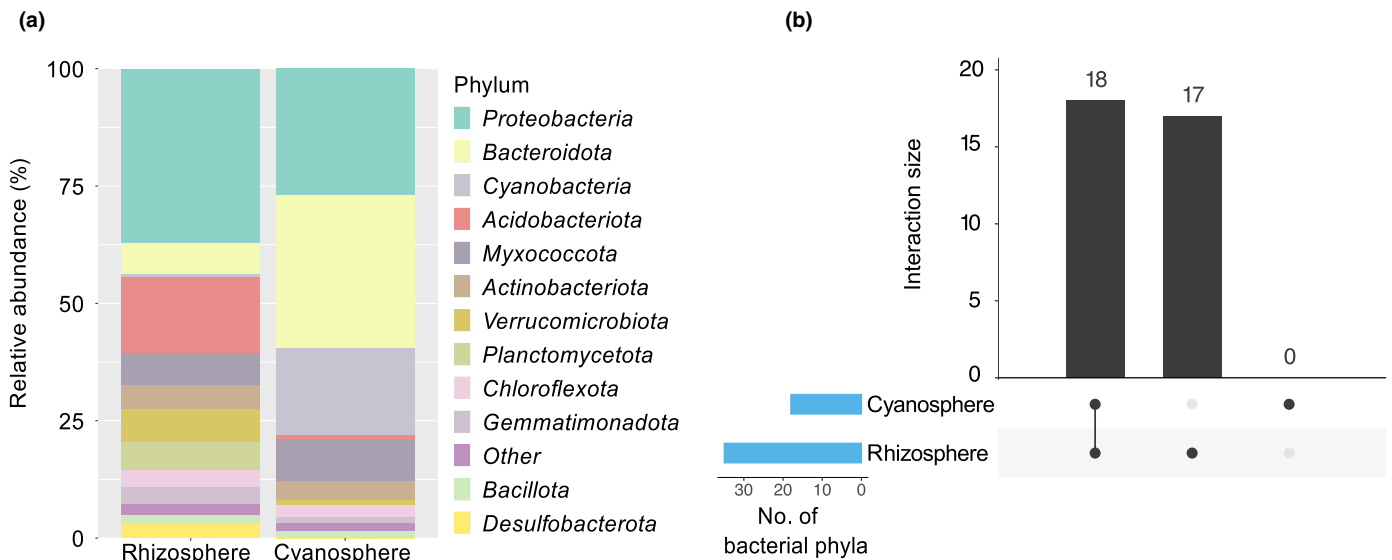


**Fig. 1** Comparison of mean relative abundances of bacterial/archaeal phyla in the rhizosphere and the cyanosphere. (a) Relative abundance of the bacterial communities identified in the rhizosphere (181 samples) and the cyanosphere (40 samples) at the phylum level based on retrospective data analysis. Data represent the mean relative abundance of all 181 samples in the rhizosphere or 40 samples in the cyanosphere. (b) UpSet plot showing the quantitative intersection of the shared and unique bacterial phyla in the cyanosphere and the rhizosphere. All 18 bacterial phyla present in the cyanosphere were also present in the rhizosphere and the rhizosphere contains 17 bacterial phyla not in the cyanosphere.

water as an inoculant. Here, we collected the roots of the model plant (*B. distachyon*) after 5 d of inoculation to avoid moisture damage to plant leaves caused by touching the inner wall of the EcoFABs. The dominant biocrust cyanobacterium (*M. vaginatus*) was grown in a dedicated growth chamber and was harvested after 14 d of inoculation with biocrust soil water. The DNA of the biocrust inoculum and each inoculated host was extracted and subjected to 16S rRNA gene amplification and sequencing.

Nineteen bacterial phyla were found in the biocrust inoculum, with *Proteobacteria*, *Bacteroidota*, *Actinobacteriota*, and *Cyanobacteria* accounting for > 80% of sequences (Fig. 2a; Tables S5, S6). *Microcoleus vaginatus* and other 12 ASVs belonging to *Cyanobacteria* were found in the biocrust inoculum, including two other *Microcoleus*, *Phormidium*, *Tychonema*, and *Wilmottla* (Table S5). However, no *Cyanobacteria* were recruited to both hosts which may be due to potential nutrient competition between these

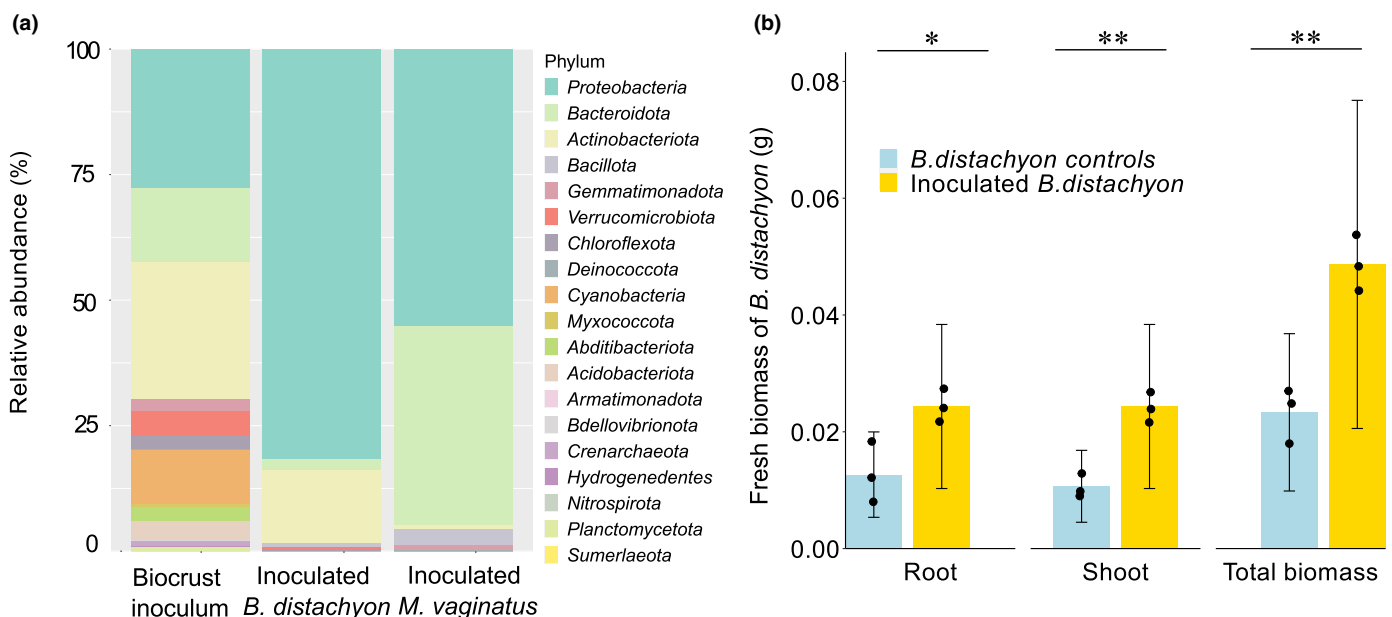


**Fig. 2** Hosts inoculated by biocrust communities ( $n = 3$ ). (a) Relative abundance of the biocrust bacterial/archaeal communities in the inoculum and recruited to *Brachypodium distachyon* and *Microcoleus vaginatus* at the phylum level; data represent the mean of three replicate samples. Values for each replicate are available in Supporting Information Table S6. (b) Root biomass, shoot biomass, and total biomass production of *B. distachyon* after 5 d of inoculation by the biocrust soil water. The points represent the values of individual samples. The error bars are SE. Significance levels of biomass differences between inoculated plants and uninoculated controls were obtained with Welch's *t*-tests: \*,  $P < 0.05$ ; \*\*,  $P < 0.01$ .

*Cyanobacteria* and other microbial species, as well as competition between *Cyanobacteria* and the hosts within the hydroponic systems. This also revealed that *B. distachyon* and *M. vaginatus* recruited a total of 7 and 8 bacterial phyla, respectively (Fig. 2a), of which, *Proteobacteria*, *Bacteroidota*, *Actinobacteriota*, and *Bacillota* were recruited to both hosts. *Proteobacteria* and *Bacteroidota* accounted for almost 90% of sequences recruited to both *B. distachyon* and *M. vaginatus*. *Chloroflexota* and *Myxococcota* were only found to be associated with *B. distachyon*, while *Cyanobacteria*, *Deinococcota*, and *Gemmatimonadota* were only recruited to *M. vaginatus*. Notably, various putative plant growth-promoting bacteria (PGPB) were recruited to both *B. distachyon* and *M. vaginatus*, including seven families of *Proteobacteria* and one family of *Bacteroidota*, that is, *Rhodanobacteraceae*, *Beijerinckiaceae*, *Caulobacteraceae*, *Pleomorphomonadaceae*, *Comamonadaceae*, and *Cytophagaceae* (Table S5). Consistent with our retrospective study, microbes recruited to our plant/cyanobacterial hosts are substantially different at the ASV level (Fig. S4).

Notably, *B. distachyon* inoculation with the biocrust soil water resulted in higher root, shoot, and total biomass (Fig. 2b) by 1.9-, 2.2-, and 2.1-fold, respectively. By contrast, *M. vaginatus* Chla fluorescence, an indicator of cyanobacterium growth, did not change significantly ( $P=0.45$ ) after 14 d of inoculation compared with uninoculated controls (Fig. S5). These results suggest that either the soil extract contained microbes, nutrients, and/or metabolites that were needed by the plant and not the cyanobacterial host, or the extracts contained cyanobacterial inhibitors as well as promoters which resulted in a neutral effect on cyanobacterial hosts. It is also possible there are different interactions between native biocrust cyanobacteria and the isolates *M. vaginatus* strain used in this study.

### Three Biocrust isolates promoted the growth of both *B. distachyon* and *M. vaginatus*

Given the observed growth promotion of *B. distachyon* by the soil water from biocrusts, we next examined growth promotion by individual biocrust isolates from an existing collection (da Rocha *et al.*, 2015). To do this, we selected 18 bacterial isolates (Table 1) based on our 16S rRNA gene sequencing data and performed a host–microbe co-culture experiment using individual biocrust isolates to inoculate the root of *B. distachyon* and cultures of *M. vaginatus*.

Each *B. distachyon* was harvested after 14 d of inoculation by isolates when it reached the inner wall of the EcoFABs. After 14 d of inoculation of *B. distachyon*, by washing host tissues using  $1 \times$  PBS, and subsequently plating an aliquot (15  $\mu$ l) of the washed solution onto  $1 \times$  R2A agar plates, we found that 15 of 17 isolates (*Modestobacter versicolor*\_D2B23 was excluded due to contamination) survived in the media; *Micromonospora* sp.\_D2D21 and *Paracraurococcus* sp.\_L1B40 were the exceptions. Overall, three isolates (*Bosea* sp.\_L1B56, *Pseudarthrobacter* sp.\_L1D14, and *Pseudarthrobacter picheli*\_L1D33) positively influenced the total biomass production of *B. distachyon* (Fig. 3).

We also evaluated the different effects of the isolates on the root and shoot biomass and found shoot biomass was increased

(74%) after inoculation with *Pseudarthrobacter picheli*\_L1D33. Other observations include, that root biomass was increased between 128% and 381% by *Solirubrobacter* sp.\_L1B27, *Bosea* sp.\_L1B56, *Pseudarthrobacter* sp.\_L1D14, *Pseudarthrobacter picheli*\_L1D33, and *Belnapia moabensis*\_D1B50 (Fig. S6). Meanwhile, all tested biocrust bacterial isolates survived in the media after 14 d of inoculation of *M. vaginatus* but showed different effects on host growth, that is, positive, neutral, or negative. Nine out of 17 isolates including *Bosea* sp.\_L1B56, *Pseudarthrobacter* sp.\_L1D14, and *Pseudarthrobacter picheli*\_L1D33 significantly promoted *M. vaginatus* growth to an extent of 50–70%; three isolates (*Paracraurococcus* sp.\_L1B40, *Micromonospora* sp.\_D2D21, and *Arthrobacter oryzae*\_L1B36) showed no growth-promoting effects, and the remaining five isolates exerted a negative effect on the biomass production of *M. vaginatus* (Fig. 3).

When comparing the host growth promotion effects, we find that the responses of *B. distachyon* and *M. vaginatus* to most isolates are not highly correlated ( $R^2=0.05$ ; Fig. S7), but *Bosea* sp.\_L1B56, *Pseudarthrobacter* sp.\_L1D14, and *Pseudarthrobacter picheli*\_L1D33 showed a consistent promotion effect on the biomass production of both hosts (Fig. 3).

### Metabolites mediate beneficial plant–microbe interactions

To determine whether biocrust isolates secrete metabolites that potentially promote the growth of the photoautotrophic hosts, we used exometabolomics (Baran *et al.*, 2015) and conducted LC–MS/MS analysis of exometabolites of biocrust isolates grown in a medium made of exudates from *B. distachyon* root or *M. vaginatus*, which revealed that a cocktail of chemicals that vary in composition, including nucleotides, amino acids, organic acids, sugars, and vitamins (Table S3), was secreted by roots of *B. distachyon* and *M. vaginatus*. The peak height of these metabolites in uninoculated controls can be seen in Fig. S8.

All 18 biocrust isolates consumed aspartic acid but secreted dihydroxybenzoic acid when grown in root exudates of *B. distachyon* (Fig. S9a), while they consumed hypoxanthine, guanosine, *N*-acetyl-glutamic acid, and *N*-alpha-acetyl-lysine and secreted thymine and malonic acid when grown in *M. vaginatus* exudates (Fig. S9b). Among all metabolites, 2'-deoxyadenosine, adenine, hypoxanthine, deoxycytidine, 2'-deoxyguanosine, cytidine, guanosine, methionine, proline, lysine, agmatine sulfuric acid, valine, alanine, and citrulline were consumed by all three PGPB while thymine, indole-3-acetic acid, and dihydroxybenzoic acids were secreted when they were grown in both hosts' exudates (Fig. S9). Moreover, the metabolites consumption/secretion patterns showed some clustering by phylogeny in both hosts' exudates (Fig. S10).

After comparing the abundance of metabolites secreted by PGPB and by the other tested isolates, we found pantothenic acid was the only metabolite secreted by PGPB that was relatively higher in PGPB than in controls when grown in both hosts' exudates. Although both hosts secreted some pantothenic acid (PA), the levels of pantothenic acid were found to increase in spent media of *Pseudarthrobacter* sp.\_L1D14 and *Pseudarthrobacter picheli*\_L1D33 grown in hosts' exudates (Fig. 4a). To further



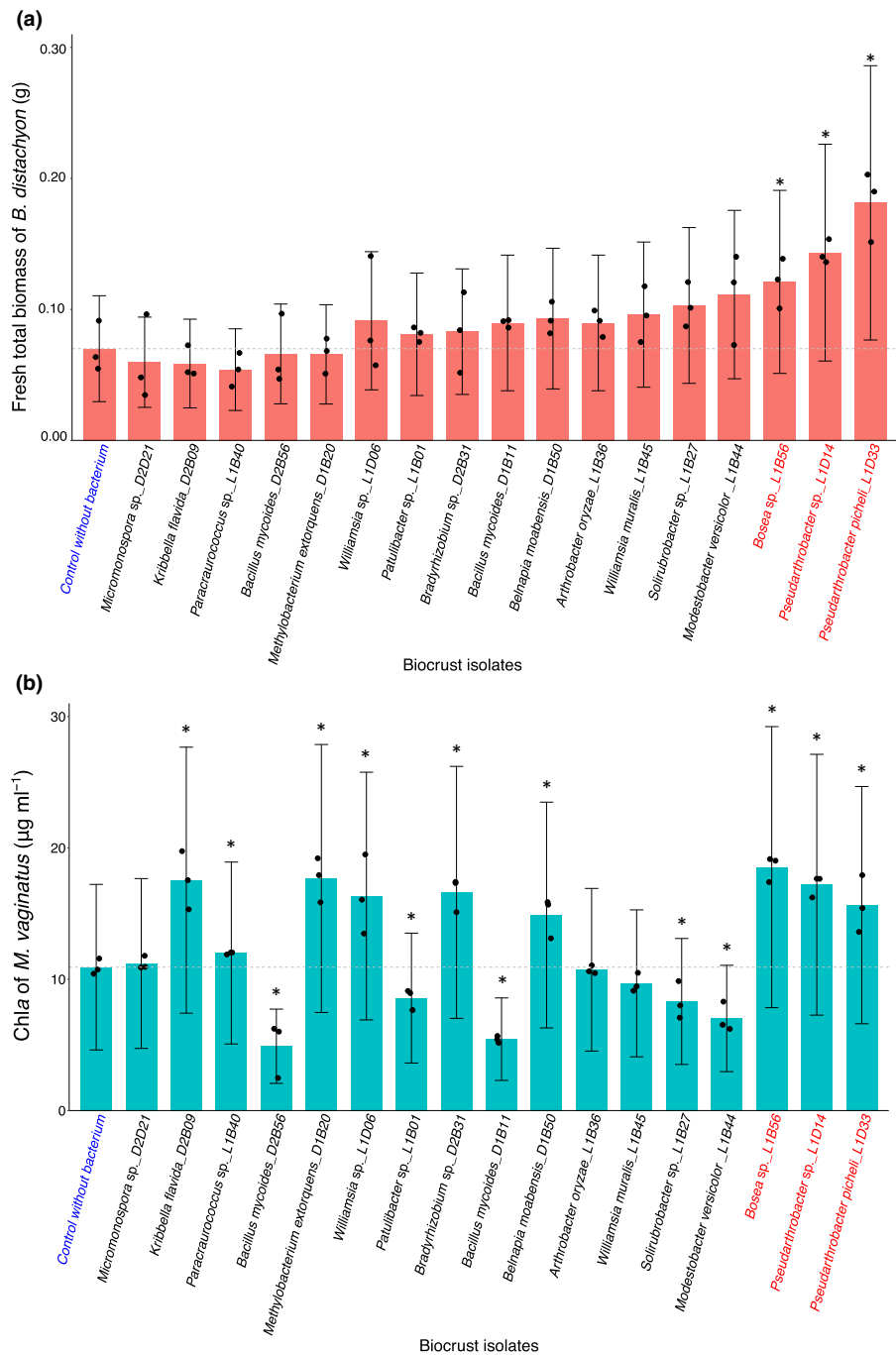


**Fig. 3** Total biomass production of (a) *Brachypodium distachyon* and (b) *Microcoleus vaginatus* after 14 d of inoculation by individual biocrust isolates ( $n = 3$ ). The points represent the values of individual samples. The error bars are SE. The gray dashed line represents the mean value of uninoculated controls. The red-highlighted x-axial labels represent biocrust isolates that promote the growth of both hosts, and the blue-highlighted x-axial label represents control samples without bacterium. Significance levels of biomass differences between inoculated hosts and uninoculated controls were obtained by Welch's  $t$ -tests: \*,  $P < 0.05$ .

investigate the effect of pantothenic acid on host biomass production, we cultivated *B. distachyon* and *M. vaginatus* in media supplemented with several different concentrations with PA, including 0.01  $\mu\text{M}$ , 0.1  $\mu\text{M}$ , 1  $\mu\text{M}$ , 0.01 mM, and 0.1 mM PA, based on literature values (Williams & Rohrman, 1935), and compared the biomass production with the controls. We collected each *B. distachyon* after 28 d supplemented with pantothenic acid when it reached the edge of the culture plates. We found a significant growth-promoting effect of PA on *B. distachyon* with 0.01  $\mu\text{M}$  PA, with no significant effect on *M. vaginatus* biomass 28 d of cultivation (Fig. 4b).

## Discussion

Plant roots and the biocrust cyanobacterium *M. vaginatus* have been known to release metabolites that play key roles in mediating plant–microbe interactions, for example, by improving the root microenvironment to recruit beneficial bacterial partners or suppressing pathogens (Walker *et al.*, 2003; Rodríguez-Celma *et al.*, 2013; Baran *et al.*, 2015; Zhalnina *et al.*, 2018). In this study, we investigated beneficial host–bacteria interactions in both the rhizosphere and the cyanosphere. Specifically, we compared microbiomes in the rhizosphere and the cyanosphere by

analyzing retrospective 16S rRNA gene sequencing data, conducting host inoculation experiments with biocrust communities and isolates, performing exometabolite profiling, and evaluating the effect of metabolites on host biomass production. To our knowledge, this is the first study revealing bacterial growth promotion across these two domains of photoautotrophs.

Our retrospective analysis showed that all 18 microbial phyla found in the cyanosphere were also present in the rhizosphere, and 17 phyla were present in the rhizosphere but not the cyanosphere (Fig. 1b), consistent with lower bacterial diversity typically detected in biocrusts than in soils (da Rocha *et al.*, 2015; Fitzpatrick *et al.*, 2018). Among the shared microbes, *Proteobacteria* and *Bacteroidota* were abundant in both the rhizosphere and the cyanosphere, in line with previous findings showing them as members of the 'core microbiome' in the rhizosphere of diverse grass species (Naylor *et al.*, 2017; Pickett *et al.*, 2021). This is likely due to their ability to invade and persist outside the roots of distinct plant species (Hacquard *et al.*, 2015) and cyanobacteria. Niche adaptation (e.g. to nutrient availability) may also explain the prevalence of these taxonomic groups in the rhizosphere and the cyanosphere as they were typically considered copiotrophs adapted to C-rich conditions (common in both environments; Hacquard *et al.*, 2015; Ling *et al.*, 2022). As studies on the biocrust cyanosphere have only emerged recently, there are limited public datasets on cyanosphere microbiomes available for our comparisons. Yet, our findings confirmed the presence of shared bacterial phyla in the rhizosphere and cyanosphere, though they are substantially different at the ASV level.

Host inoculation experiments with biocrust soil water revealed significant growth promotion for *B. distachyon* (Fig. 2b) but not *M. vaginatus* (Fig. S5), the opposite of what was hypothesized. Given subsequent observations that biocrust isolates can promote *M. vaginatus* growth (Fig. 3), this observation either suggests that the growth-promoting bacteria were not recruited in this portion of the study, possibly due to competition with other microorganisms, or suggests competing positive and negative effects of recruited microbes. Although there are differences in recruited microbiomes by both hosts, our host inoculation experiments with biocrust soil water showed that *Proteobacteria* and *Bacteroidota* were dominant phyla recruited to both *B. distachyon* root and *M. vaginatus*. This included a set of putative PGPB (such as members from the *Comamonadaceae* family). *Proteobacteria* and *Bacteroidota* have also been found to be associated with the roots of diverse grass species, including *Brachypodium distachyon*, *Zea mays*, *Sorghum* sp., and *Triticum* sp. (Donn *et al.*, 2015; Kawasaki *et al.*, 2016; Naylor *et al.*, 2017). Our host inoculation experiments revealed clear differences at the ASV level yet with many of the same phyla of bacteria recruited to both hosts, consistent with our retrospective data analysis.

To investigate strain-specific host growth promotion, we inoculated *B. distachyon* roots and *M. vaginatus* with diverse individual biocrust isolates. Intriguingly, we observed that the same bacterial isolates promoted host growth in both prokaryotic and eukaryotic hosts. Specifically, three isolates including *Bosea* sp.\_L1B56, *Pseudarthrobacter* sp.\_L1D14, and *Pseudarthrobacter picheli*\_L1D33 successfully promoted biomass production in

both hosts after inoculation (Figs 3, S6). As one of the most frequently soil-isolated *Actinobacteriota*, *Pseudarthrobacter* has been previously reported to promote plant growth. For example, *Pseudarthrobacter oxydans* SBA82 was reported to increase the shoot biomass yield of different types of plants (Ghasemi *et al.*, 2018). *Pseudarthrobacter* sp. NIBRBAC000502770 was found to produce a high amount of indole acetic acid which promotes plant growth (Ham *et al.*, 2021). *Bosea* species have been isolated from lupin root nodules (De Meyer & Willems, 2012) and identified from wheat rhizosphere soil (Rilling *et al.*, 2018) and are typically recognized as nitrogen-fixing heterotrophic bacteria associated with plants; possibly, the observed host growth promotion by *Bosea* may involve nitrogen fixation, and other effects such as local environmental conditions (e.g. O<sub>2</sub> concentrations or host growth-promoting related genes expression) may be additional factors. Such PGPB found in the rhizosphere may enhance plant growth directly, by facilitating nutrient acquisition or modulating plant hormone levels, or indirectly, by protecting plants from pathogens and abiotic stresses (Glick, 1995; De Souza *et al.*, 2015).

Exometabolomic analysis was performed to provide additional insights into bacterial recruitment and growth promotion effects. Both *B. distachyon* and *M. vaginatus* exudates comprise a broad range of metabolites, including nucleotides, amino acids, organic acids, sugars, and vitamins (Table S3). Exometabolite profiles of all bacterial isolates grown in both hosts' exudates were clustered by bacterial phylogeny (Fig. S10). This is consistent with previous studies showing two model strains of *Roseobacter* secreting a similar set of metabolites that may help the growth of marine microbes (Wienhausen *et al.*, 2017), as well as two *Streptomyces* strains that shared core metabolites (Sottorff *et al.*, 2019). In our study, a set of metabolites that include 2'-deoxyadenosine, adenine, hypoxanthine, deoxycytidine, 2'-deoxyguanosine, cytidine, guanosine, methionine, proline, lysine, agmatine sulfuric acid, valine, alanine, and citrulline were secreted by both hosts and were consumed by all 3 PGPB (*Bosea* sp.\_L1B56, *Pseudarthrobacter* sp.\_L1D14 and *Pseudarthrobacter picheli*\_L1D33), suggesting similar host-microbe interactions and a possible common recruitment mechanism via similar compounds exudation by both hosts. This was also observed in the synthetic phycosphere of marine phytoplankton, where photosynthetic hosts recruit beneficial bacteria through the secretion of metabolites (Fu *et al.*, 2020).

Two of the *Actinobacteria* tested in this study (*Pseudarthrobacter* sp.\_L1D14 and *Pseudarthrobacter picheli*\_L1D33) promoted biomass production in either host. Excitingly, these two plant and cyanobacteria growth-promoting *Pseudarthrobacter* were found to secrete pantothenic acid when growing in both hosts' exudates. Pantothenic acid is a water-soluble vitamin that is a precursor in the synthesis of coenzyme A produced by plants, bacteria, and molds (Marek-Kozaczuk & Skorupska, 2001). The stimulative effect of pantothenic acid on plant growth has been reported earlier, including on the growth of alfalfa seedlings (a flowering plant), Lemna (a free-floating aquatic plant), potatoes, *Ricciocarpos natans*, and other green plants (Williams *et al.*, 1933; McBurney *et al.*, 1935; Williams & Rohrman, 1935).

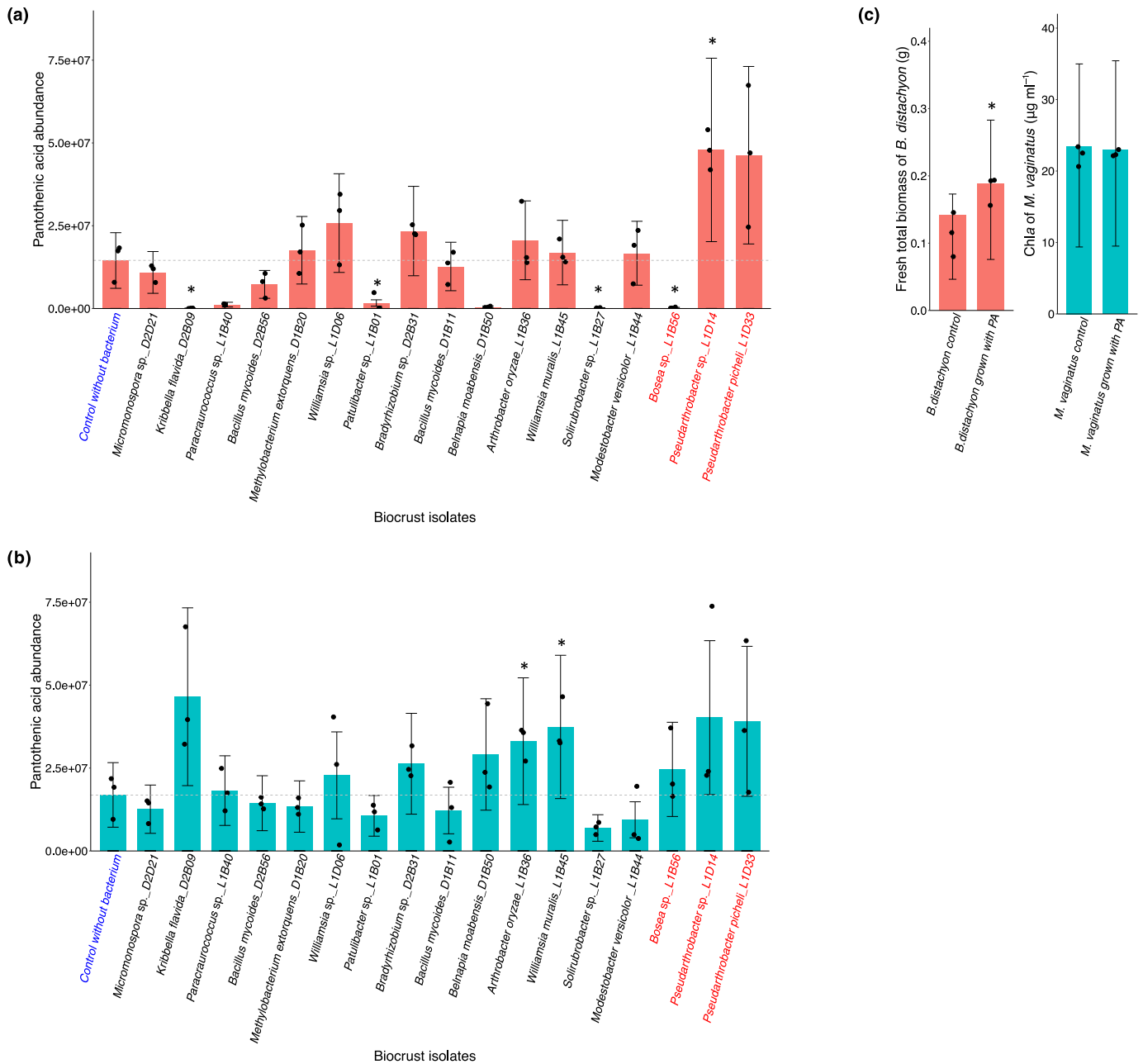


**Fig. 4** Pantothenic acid (PA) production by individual isolates cultured on hosts' exudates ( $n = 3$ ). PA relative abundance (peak height) detected in spent media collected from exudates of (a) *Brachypodium distachyon* or (b) *Microcoleus vaginatus* with growing biocrust isolates. Pantothenic acid in control samples is produced by hosts. The red-highlighted x-axis labels represent biocrust isolates that promote the growth of both hosts, and the blue-highlighted x-axis label represents control samples without bacterium. PA effect on host growth. Significance levels obtained by Welch's  $t$ -tests reflect the difference of PA signal in spent media collected from inoculated hosts compared with uninoculated controls: \*,  $P < 0.05$ . (c) Total biomass production of *B. distachyon* or *M. vaginatus* after growing on  $0.2 \times$  MS agar or  $1 \times$  BG11 medium supplemented with or without  $0.01 \mu\text{M}$  PA for 28 d. The points represent the values of individual samples. The error bars are SE. The gray dashed line represents the mean value of uninoculated controls. Significance levels of host biomass production in media supplemented with PA compared with controls without PA in growing media were obtained by Welch's  $t$ -tests: \*,  $P < 0.05$ .

Subsequent plant and cyanobacteria growth studies with *B. distachyon* and *M. vaginatus* revealed that this compound resulted in a 60% increase in *B. distachyon* biomass but no increase in *M. vaginatus* biomass after 28 d. There are many possible explanations for the lack of growth promotion by pantothenic acid. The concentrations could be too low, other factors may be limiting or

another process such as nitrogen fixation explains the growth promotion observed in our co-culture study. For example, members of *Arthrobacter* and *Bacillus* were found to fix nitrogen and promote the growth of *M. vaginatus* in a co-culture experiment (Nelson *et al.*, 2021). Based on this and the observed positive impact of pantothenic acid on *B. distachyon* and not *M. vaginatus*,

increased nitrogen availability may be an important benefit to the non-diazotrophic cyanobacterial host.

Here, we found that there were 18 shared phyla recruited by plant and cyanobacterial hosts. Given that cyanobacterial biocrusts preceded plants in colonizing lands, it is possible that plants evolved to maintain some of the beneficial interactions especially those mediated by small molecule metabolites. Consistent with this and the observed similarities in recruitment at the phylum level, we found that some bacteria benefit both hosts. Specifically, we found that three biocrust isolates (*Bosea* sp.\_L1B56, *Pseudarthrobacter* sp.\_L1D14 and *Pseudarthrobacter picheli*\_L1D33) promoted biomass production of both *B. distachyon* and *M. vaginatus* and pantothenic acid secretion by these isolates was found to promote plant growth. Overall, this suggests the potential of cyanobacteria and other diverse photoautotrophic hosts as a pool for new plant growth-promoting microbes and metabolites.

## Acknowledgements

We would like to thank Estelle Couradeau, Jacob S. Jordan, and Mia Jones for assisting with biocrust sampling, Lauren K. Jabusch and Kateryna Zhalnina for their knowledge support of EcoFABs, and Amber Golini for her help with LC–MS/MS sample analyses. This work was funded by the Office of Science Early Career Research Program, Office of Biological and Environmental Research, of the US Department of Energy under contract number DE-AC02-05CH11231 to Lawrence Berkeley National Laboratory and the ECON Project supported by the Office of Science, Office of Biological and Environmental Research, the US Department of Energy grant no. DE-SC0021369 to Montana State University.








## Competing interests

None declared.

## Author contributions

QZ and TRN planned and designed the research. QZ and YH conducted experiments. QZ, YH, SMK, MWVG and BPB performed data analyses. QZ, BPB and TRN wrote the paper. YH, SMK, MWVG, SGT and BPB provided comments on the manuscript.

## ORCID

Benjamin P. Bowen  <https://orcid.org/0000-0003-1368-3958>  
Yuntao Hu  <https://orcid.org/0000-0002-2409-9821>  
Suzanne M. Kosina  <https://orcid.org/0000-0003-2885-1248>  
Trent R. Northen  <https://orcid.org/0000-0001-8404-3259>  
Susannah G. Tringe  <https://orcid.org/0000-0001-6479-8427>  
Marc W. Van Goethem  <https://orcid.org/0000-0001-8688-3323>  
Qing Zheng  <https://orcid.org/0000-0002-9994-089X>

## Data availability

The raw LC–MS/MS data have been deposited in the Mass Spectrometry Interactive Virtual Environment (MassIVE) database at the Center for Computational Mass Spectrometry, University of California, San Diego under dataset number (MassIVE MSV000090897). The raw 16S rRNA gene sequence data have been submitted to NCBI and are publicly available under BioProject [PRJNA917465](https://ncbi.nlm.nih.gov/bioproject/PRJNA917465). The assembled and annotated genome of biocrust isolates is publicly available in KBase (<https://narrative.kbase.us/narrative/ws.92194.obj.1>).

The source code of the METATLAS toolbox used to obtain the extracted ion chromatograms and peak height in this study is openly available from the GitHub repository accessible at <https://github.com/biorack/metatlas>.

## References

- Abdel-Lateif K, Bogusz D, Hocher V. 2012. The role of flavonoids in the establishment of plant roots endosymbioses with arbuscular mycorrhiza fungi, rhizobia and Frankia bacteria. *Plant Signaling and Behavior* 7: 636–641.
- Baran R, Brodie EL, Mayberry-Lewis J, Hummel E, Da Rocha UN, Chakraborty R, Bowen BP, Karaoz U, Cadillo-Quiroz H, Garcia-Pichel F *et al.* 2015. Exometabolite niche partitioning among sympatric soil bacteria. *Nature Communications* 6: 1–9.
- Belnap J. 2006. The potential roles of biological soil crusts in dryland hydrologic cycles. *Hydrological Processes: An International Journal* 20: 3159–3178.
- Belnap J, Weber B, Büdel B. 2016. *Biological soil crusts: an organizing principle in drylands*. Cham, Switzerland: Springer, 3–13.
- Benjamini Y, Hochberg Y. 1995. Controlling the false discovery rate: a practical and powerful approach to multiple testing. *Journal of the Royal Statistical Society* 57: 289–300.
- Bowen BP, Northen TR. 2010. Dealing with the unknown: metabolomics and metabolite atlases. *Journal of the American Society for Mass Spectrometry* 21: 1471–1476.
- Bressan M, Roncato MA, Bellvert F, Comte G, Haichar FEZ, Achouak W, Berge O. 2009. Exogenous glucosinolate produced by *Arabidopsis thaliana* has an impact on microbes in the rhizosphere and plant roots. *The ISME Journal* 3: 1243–1257.
- Callahan BJ, McMurdie PJ, Rosen MJ, Han AW, Johnson AJ, Holmes SP. 2016. DADA2: high-resolution sample inference from Illumina amplicon data. *Nature Methods* 13: 581–583.
- Caporaso JG, Lauber CL, Walters WA, Berg-Lyons D, Huntley J, Fierer N, Owens SM, Betley J, Fraser L, Bauer M *et al.* 2012. Ultra-high-throughput microbial community analysis on the Illumina HiSeq and MiSeq platforms. *The ISME Journal* 6: 1621–1624.
- Chamizo S, Cantón Y, Rodríguez-Caballero E, Domingo F. 2016. Biocrusts positively affect the soil water balance in semiarid ecosystems. *Ecohydrology* 9: 1208–1221.
- Coleman-Derr D, Desgarenes D, Fonseca-Garcia C, Gross S, Clingenpeel S, Woyke T, North G, Visel A, Partida-Martinez LP, Tringe SG. 2016. Plant compartment and biogeography affect microbiome composition in cultivated and native *Agave* species. *New Phytologist* 209: 798–811.
- Concostrina-Zubiri L, Huber-Sannwald E, Martínez I, Flores JF, Escudero A. 2013. Biological soil crusts greatly contribute to small-scale soil heterogeneity along a grazing gradient. *Soil Biology and Biochemistry* 64: 28–36.
- Couradeau E, Giraldo-Silva A, De Martini F, Garcia-Pichel F. 2019. Spatial segregation of the biological soil crust microbiome around its foundational cyanobacterium, *Microcoleus vaginatus*, and the formation of a nitrogen-fixing cyanosphere. *Microbiome* 7: 1–12.
- De Meyer SE, Willems A. 2012. Multilocus sequence analysis of *Bosea* species and description of *Bosea lupini* sp. nov., *Bosea lathyri* sp. nov. and *Bosea*

- robiniae* sp. nov., isolated from legumes. *International Journal of Systematic and Evolutionary Microbiology* 62: 2505–2510.
- De Souza R, Ambrosini A, Passaglia LMP. 2015. Plant growth-promoting bacteria as inoculants in agricultural soils. *Genetics and Molecular Biology* 38: 401–419.
- DeFalco LA, Detling JK, Tracy CR, Warren SD. 2001. Physiological variation among native and exotic winter annual plants associated with microbiotic crusts in the Mojave Desert. *Plant and Soil* 234: 1–14.
- Donn S, Kirkegaard JA, Perera G, Richardson AE, Watt M. 2015. Evolution of bacterial communities in the wheat crop rhizosphere. *Environmental Microbiology* 17: 610–621.
- Durán P, Flores-uribe J, Wippel K, Melkonian M, Garrido-oter R, Melkonian B. 2022. Shared features and reciprocal complementation of the *Chlamydomonas* and *Arabidopsis* microbiota. *Nature Communications* 13: 1–14.
- Elbert W, Weber B, Burrows S, Steinkamp J, Büdel B, Andreae MO, Pöschl U. 2012. Contribution of cryptogamic covers to the global cycles of carbon and nitrogen. *Nature Geoscience* 5: 459–462.
- Engelbrektson A, Kunin V, Engelbrektson A, Kunin V, Glavina del Rio T, Hugenholtz P, Tringe SG. 2012. Defining the core *Arabidopsis thaliana* root microbiome. *Nature* 488: 86–90.
- Fitzpatrick CR, Copeland J, Wang PW, Guttman DS, Kotanen PM, Johnson MTJ. 2018. Assembly and ecological function of the root microbiome across angiosperm plant species. *Proceedings of the National Academy of Sciences, USA* 115: E1157–E1165.
- Fu H, Uchimiya M, Gore J, Moran MA. 2020. Ecological drivers of bacterial community assembly in synthetic phycospheres. *Proceedings of the National Academy of Sciences, USA* 117: 3656–3662.
- Gao J, Sasse J, Lewald KM, Zhalnina K, Cormmesser LT, Duncombe TA, Yoshikuni Y, Vogel JP, Firestone MK, Northen TR. 2018. Ecosystem fabrication (EcoFAB) protocols for the construction of laboratory ecosystems designed to study plant–microbe interactions. *Journal of Visualized Experiments* 2018: 1–16.
- García-Pichel F, Wojciechowski MF. 2009. The evolution of a capacity to build supra-cellular ropes enabled filamentous cyanobacteria to colonize highly erodible substrates. *PLoS ONE* 4: 4–9.
- Ghasemi Z, Ghaderian SM, Rodríguez-Garrido B, Prieto-Fernández Á, Kidd PS. 2018. Plant species-specificity and effects of bioinoculants and fertilization on plant performance for nickel phytomining. *Plant and Soil* 425: 265–285.
- Glick BR. 1995. The enhancement of plant growth by free-living bacteria. *Canadian Journal of Microbiology* 41: 109–117.
- Hacquard S, Garrido-Oter R, González A, Spaepen S, Ackermann G, Lebeis S, McHardy AC, Dangl JL, Knight R, Ley R *et al.* 2015. Microbiota and host nutrition across plant and animal kingdoms. *Cell Host and Microbe* 17: 603–616.
- Ham S, Yoon H, Park JM, Park YG. 2021. Optimization of fermentation medium for indole acetic acid production by *Pseudarthrobacter* sp. NIBRBAC000502770. *Applied Biochemistry and Biotechnology* 193: 2567–2579.
- Hamonts K, Trivedi P, Garg A, Janitz C, Grinyer J, Holford P, Botha FC, Anderson IC, Singh BK. 2018. Field study reveals core plant microbiota and relative importance of their drivers. *Environmental Microbiology* 20: 124–140.
- Havrilla CA, Chaudhary VB, Ferrenberg S, Antoninka AJ, Belnap J, Bowker MA, Eldridge DJ, Faist AM, Huber-Sannwald E, Leslie AD *et al.* 2019. Towards a predictive framework for biocrust mediation of plant performance: a meta-analysis. *Journal of Ecology* 107: 2789–2807.
- Hu L, Robert CAM, Cadot S, Zhang X, Ye M, Li B, Manzo D, Chervet N, Steinger T, Van Der Heijden MGA *et al.* 2018. Root exudate metabolites drive plant–soil feedbacks on growth and defense by shaping the rhizosphere microbiota. *Nature Communications* 9: 1–13.
- Kawasaki A, Donn S, Ryan PR, Mathesius U, Devilla R, Jones A, Watt M. 2016. Microbiome and exudates of the root and rhizosphere of *Brachypodium distachyon*, a model for wheat. *PLoS ONE* 11: e0164533.
- Konstantinidis KT, Tiedje JM. 2005. Genomic insights that advance the species definition for prokaryotes. *Proceedings of the National Academy of Sciences, USA* 102: 2567–2572.
- Kudjordjie EN, Sapkota R, Steffensen SK, Fomsgaard IS, Nicolaisen M. 2019. Maize synthesized benzoxazinoids affect the host associated microbiome. *Microbiome* 7: 1–17.
- Lemanceau P, Blouin M, Muller D, Moëgne-Loccoz Y. 2017. Let the core microbiota be functional. *Trends in Plant Science* 22: 583–595.
- Lesica P, Shelly JS. 1992. Effects of cryptogamic soil crust on the population dynamics of *Arabis fecunda* (Brassicaceae). *American Midland Naturalist* 128: 53–60.
- Ling N, Wang T, Kuzyakov Y. 2022. Rhizosphere bacteriome structure and functions. *Nature Communications* 13: 1–13.
- Marek-Kozaczuk M, Skorupska A. 2001. Production of B-group vitamins by plant growth-promoting *Pseudomonas fluorescens* strain 267 and the importance of vitamins in the colonization and nodulation of red clover. *Biology and Fertility of Soils* 33: 146–151.
- McBurney CH, Bollen WB, Williams RJ. 1935. Pantothenic acid and the nodule bacteria–legume symbiosis. *Proceedings of the National Academy of Sciences, USA* 21: 301–304.
- Naylor D, Degraaf S, Purdom E, Coleman-Derr D. 2017. Drought and host selection influence bacterial community dynamics in the grass root microbiome. *The ISME Journal* 11: 2691–2704.
- Nelson C, Garcia-Piche F. 2021. Beneficial cyanosphere heterotrophs accelerate establishment. *Applied and Environmental Microbiology* 87: e01236.
- Nelson C, Giraldo-Silva A, Garcia-Pichel F. 2021. A symbiotic nutrient exchange within the cyanosphere microbiome of the biocrust cyanobacterium, *Microcoleus vaginatus*. *The ISME Journal* 15: 282–292.
- Pickett B, Carey CJ, Arogyaswamy K, Botthoff J, Maltz M, Catalán P, Aronson EL. 2021. Enriched root bacterial microbiome in invaded vs native ranges of the model grass allotetraploid *Brachypodium hybridum*. *Biological Invasions* 4: 1097–1116.
- R Core Team. 2019. *R: a language and environment for statistical computing*. Vienna, Austria: R Foundation for Statistical Computing. [WWW document] URL <https://www.R-project.org/> [accessed 15 December 2019].
- Rilling JI, Acuña JJ, Sadowsky MJ, Jorquera MA. 2018. Putative nitrogen-fixing bacteria associated with the rhizosphere and root endosphere of wheat plants grown in an andisol from southern Chile. *Frontiers in Microbiology* 9: 1–13.
- Ritchie RJ. 2006. Consistent sets of spectrophotometric chlorophyll equations for acetone, methanol and ethanol solvents. *Photosynthesis Research* 89: 27–41.
- da Rocha UN, Cadillo-Quiroz H, Karaoz U, Rajeev L, Klitgord N, Dunn S, Truong V, Buenrostro M, Bowen BP, Garcia-Pichel F *et al.* 2015. Isolation of a significant fraction of non-phototroph diversity from a desert biological soil crust. *Frontiers in Microbiology* 6: 1–14.
- Rodríguez-Caballero E, Belnap J, Büdel B, Crutzen PJ, Andreae MO, Pöschl U, Weber B. 2018. Dryland photoautotrophic soil surface communities endangered by global change. *Nature Geoscience* 11: 185–189.
- Rodríguez-Celma J, Lin WD, Fu GM, Abadía J, López-Millán AF, Schmidt W. 2013. Mutually exclusive alterations in secondary metabolism are critical for the uptake of insoluble iron compounds by *Arabidopsis* and *Medicago truncatula*. *Plant Physiology* 162: 1473–1485.
- Sasse J, Martinoia E, Northen T. 2018. Feed your friends: do plant exudates shape the root microbiome? *Trends in Plant Science* 23: 25–41.
- Sottorff I, Wiese J, Lipfert M, Preußke N, Sönnichsen FD, Imhoff JF. 2019. Different secondary metabolite profiles of phylogenetically almost identical *Streptomyces griseus* strains originating from geographically remote locations. *Microorganisms* 7: 166.
- Strauss SL, Day TA, Garcia-Pichel F. 2012. Nitrogen cycling in desert biological soil crusts across biogeographic regions in the Southwestern United States. *Biogeochemistry* 108: 171–182.
- Swenson TL, Karaoz U, Swenson JM, Bowen BP, Northen TR. 2018. Linking soil biology and chemistry in biological soil crust using isolate exometabolomics. *Nature Communications* 9: 19.
- Tucker CL, McHugh TA, Howell A, Gill R, Weber B, Belnap J, Grote E, Reed SC. 2017. The concurrent use of novel soil surface microclimate measurements to evaluate CO<sub>2</sub> pulses in biocrusted interspaces in a cool desert ecosystem. *Biogeochemistry* 135: 239–249.
- Vogel J, Hill T. 2008. High-efficiency *Agrobacterium*-mediated transformation of *Brachypodium distachyon* inbred line Bd21-3. *Plant Cell Reports* 27: 471–478.

- van de Voorde TFJ, van der Putten WH, Bezemer TM. 2012. Soil inoculation method determines the strength of plant–soil interactions. *Soil Biology and Biochemistry* 55: 1–6.
- Walker TS, Bais HP, Grotewold E, Vivanco JM. 2003. Root exudation and rhizosphere biology. *Plant Physiology* 132: 44–51.
- Wang Q, Garrity GM, Tiedje JM, Cole JR. 2007. Naïve Bayesian classifier for rapid assignment of rRNA sequences into the new bacterial taxonomy. *Applied and Environmental Microbiology* 73: 5261–5267.
- Wienhausen G, Noriega-Ortega BE, Niggemann J, Dittmar T, Simon M. 2017. The exometabolome of two model strains of the *Roseobacter* group: a marketplace of microbial metabolites. *Frontiers in Microbiology* 8: 1–15.
- Williams RJ, Lyman CM, Goodyear GH, Truesdail JH, Holaday D. 1933. “Pantothenic acid,” a growth determinant of universal biological occurrence. *Journal of the American Chemical Society* 55: 2912–2927.
- Williams RJ, Rohman E. 1935. Pantothenic acid as a nutrilit for green plants. *Plant Physiology* 10: 559–563.
- Xu J, Zhang Y, Zhang P, Trivedi P, Riera N, Wang Y, Liu X, Fan G, Tang J, Coletta-Filho HD *et al.* 2018. The structure and function of the global citrus rhizosphere microbiome. *Nature Communications* 9: 4894.
- Yao Y, Sun T, Wang T, Ruebel O, Northen T, Bowen BP. 2015. Analysis of metabolomics datasets with high-performance computing and metabolite atlases. *Metabolites* 5: 431–442.
- Yeoh YK, Dennis PG, Paungfoo-Lonhienne C, Weber L, Brackin R, Ragan MA, Schmidt S, Hugenholtz P. 2017. Evolutionary conservation of a core root microbiome across plant phyla along a tropical soil chronosequence. *Nature Communications* 8: 215.
- Zhalnina K, Louie KB, Hao Z, Mansoori N, Da Rocha UN, Shi S, Cho H, Karaoz U, Loqué D, Bowen BP *et al.* 2018. Dynamic root exudate chemistry and microbial substrate preferences drive patterns in rhizosphere microbial community assembly. *Nature Microbiology* 3: 470–480.
- Zhang YM, Nie HL. 2011. Effects of biological soil crusts on seedling growth and element uptake in five desert plants in Junggar Basin, western China. *Chinese Journal of Plant Ecology* 35: 380–388.
- Zheng Q, Hu Y, Zhang S, Noll L, Böckle T, Richter A, Wanek W. 2019. Growth explains microbial carbon use efficiency across soils differing in land use and geology. *Soil Biology and Biochemistry* 128: 45–55.
- Zhou X, Wu F. 2012. *p*-Coumaric acid influenced cucumber rhizosphere soil microbial communities and the growth of *Fusarium oxysporum* f.sp. *cucumerinum* Owen. *PLoS ONE* 7(10): e48288.

## Supporting Information

Additional Supporting Information may be found online in the Supporting Information section at the end of the article.

**Fig. S1** Phylogenetic tree of *Pseudarthrobacter picheli*\_L1D33 and its closely related species based on whole-genome sequencing data.

**Fig. S2** Chao1 richness and Shannon diversity of bacterial/archaeal communities in the rhizosphere ( $n = 181$ ) and the cyanosphere ( $n = 40$ ) based on retrospective data analysis.

**Fig. S3** Principal coordinates analysis plot showing microbial communities (at ASV level) in the rhizosphere ( $n = 181$ ) of different plant hosts and in the cyanosphere of *Microcoleus vaginatus* ( $n = 40$ ) of retrospective study.

**Fig. S4** Principal coordinates analysis plot showing microbes (at ASV level) in the biocrust inoculum and recruited to *Brachypodium distachyon* and *Microcoleus vaginatus* after inoculated by biocrust soil water ( $n = 3$ ).

**Fig. S5** Chla of *Microcoleus vaginatus* after 14 d of inoculation by the biocrust soil water ( $n = 3$ ).

**Fig. S6** Root and shoot biomass production of *Brachypodium distachyon* after 14 d of inoculation by individual biocrust isolates ( $n = 3$ ).

**Fig. S7** Scatter plot showing a correlation between total biomass production of *Brachypodium distachyon* and *Microcoleus vaginatus* after 14 d of inoculation by individual biocrust isolates ( $n = 3$ ).

**Fig. S8** Metabolites detected in the exudates of uninoculated hosts.

**Fig. S9** Heatmaps showing exometabolite profiles of biocrust isolates grown on both *Brachypodium distachyon* root exudates and *Microcoleus vaginatus* exudates that were measured using polar and nonpolar HPLC-MS/MS ( $n = 3$ ).

**Fig. S10** Nonmetric multidimensional scaling based on Bray–Curtis dissimilarity displaying exometabolite profiles for biocrust bacterial isolates grown in root exudates of *Brachypodium distachyon* and in exudates of *Microcoleus vaginatus* for 14 d ( $n = 3$ ).

**Table S1** Details of studies included in the retrospective study.

**Table S2** LC–MS/MS parameters.

**Table S3** Metabolites identification table.

**Table S4** Mean relative abundance (%) of bacterial/archaeal phyla in the rhizosphere and the cyanosphere based on retrospective data analysis.

**Table S5** Taxonomy and relative abundance (%) of bacterial/archaeal present in biocrust inoculum or recruited to *Brachypodium distachyon* and *Microcoleus vaginatus* after being inoculated by the biocrust soil water.

**Table S6** Relative abundance (%) of bacterial/archaeal phyla recruited to *Brachypodium distachyon* and *Microcoleus vaginatus* after being inoculated by the biocrust soil water.

Please note: Wiley is not responsible for the content or functionality of any Supporting Information supplied by the authors. Any queries (other than missing material) should be directed to the *New Phytologist* Central Office.